5. Interstellar Helium Glow

Experiment MA-088

S. Bowyer,[a†] J. Freeman,[a] M. Lampton,[a] and F. Paresce[a]

ABSTRACT

A four-channel photometer sensitive to two solar extreme-ultraviolet lines that are resonantly scattered by helium gas was developed for the Apollo-Soyuz Test Project. Two channels were used to observe the 58.4-nm line of He I (neutral), and helium gas resonant absorption cells were used to determine the intensities of the center and wings of that line. The other two channels were used to observe the 30.4-nm line of the He II (singly ionized).

The instrument surveyed much of the celestial sphere during a series of slow rolling maneuvers by the Apollo spacecraft. The experiment operated properly and usable data were obtained. Study of the distributions of observed flux and study of the ratio of 58.4-nm fluxes observed with gas cells full and empty will refine current understanding of several poorly known properties of the local interstellar medium. Study of the 30.4-nm flux distribution will refine present knowledge of the structure of the Earth's plasmasphere.

INTRODUCTION

Observation of interstellar gas passing through the solar system provides information about the temperature, number density, and bulk velocity of the local interstellar medium (ISM). As discussed by Danby and Camm (ref. 5-1), Blum and Fahr (ref. 5-2), Holzer and Axford (ref. 5-3), Axford (ref. 5-4), Johnson (ref. 5-5), and Wallis (ref. 5-6), neutral atoms passing near the Sun are gravitationally focused into a density distribution for which the shape depends, in a complicated manner, both on ISM parameters and on the local effects of photoionization by the Sun, collisional ionization by the solar wind, collisions with other atoms, and the pressure of sunlight. Detailed study of this density distribution permits untangling of the various parameters, some of which are uncertain by an order of magnitude or more. In pursuit of these ends, observations have been made of ISM hydrogen (Thomas and Krassa, ref. 5-7; Bertaux and Blamont, ref. 5-8; and Thomas, ref. 5-9) and helium (Paresce et al., refs. 5-10 and 5-11; Weller and Meier, ref. 5-12; and Freeman et al., ref. 5-13) using photometers sensitive to solar radiation resonantly scattered by the species in question.

Neutral helium is perhaps the component of the ISM most suitable for such observations, for several reasons. It is second only to neutral hydrogen in abundance, and it resonantly scatters the intense solar 58.4-nm radiation ($1s^2$—1s2p transition). This wavelength does not readily penetrate the ISM; thus, observations of local interstellar helium do not suffer, as do Lyman-α observations, from confusion from a possible galactic background flux. Finally, the Sun's gravity clearly dominates the solar radiation pressure on helium, unlike hydrogen (Fahr, ref. 5-14), resulting in sharp gravitational focusing and pronounced local helium density variations.

Any such observation made from the immediate vicinity of Earth must contend with a potentially serious background problem due to resonant

[a]University of California at Berkeley.

[†]Principal Investigator.

scattering from helium atoms in the Earth's upper atmosphere. The temperature of the helium geocorona is approximately 1000 K, (Jacchia, ref. 5-15), corresponding to helium thermal speeds of approximately 2 km/sec and to thermal-Doppler broadening of the scattered 58.4-nm line of approximately 0.6 pm full width half maximum. On the other hand, the bulk speed of the local ISM with respect to the Sun is generally believed to be 5 to 20 km/sec (Fahr, ref. 5-14; and Thomas, ref. 5-16), and the orbital speed of the Earth is 30 km/sec; hence, there are large solid angles, the configuration of which varies throughout the year, within which the radial velocities of local interstellar helium with respect to Earth are several tens of kilometers per second. This radiation will reach Earth Doppler-shifted away from the geocoronal 58.4-nm line by several times the width of that line. Hence, a narrow-band gas absorption cell having an absorption feature sufficiently wide to contain the geocoronal line will absorb the geocoronal 58.4-nm flux while transmitting most of that scattered from the local ISM. Such a cell can be made by confining helium in the optical path leading to the detector.

The intensity observed with the gas cell filled provides an additional datum that enables more detailed fitting of ISM models to observations. For the cell used in the present instrument, this signal is produced only by helium atoms moving at a radial speed of at least 9 km/sec with respect to the photometer, and is consequently a sensitive indicator of the dynamical state of the gas. The ratio ϵ_o of 58.4-nm fluxes seen with the gas cell full and empty is a particularly valuable datum because it does not depend on the integrated solar flux F at 58.4 nm, the density of helium n_{He} in the local ISM, the transmission of the broadband filters used in the photometer, or the quantum efficiency of the instrument's photon detector. Any model fitting that results from measurements of ϵ_o will therefore depend only on model parameters other than F and n_{He}, and will be independent of any changes in instrument sensitivity that may have occurred between calibration and flight. The parameter ϵ_o is clearly most useful when it can be shown that the contribution of the geocoronal 58.4-nm flux to the cell-empty count rate is small.

Observations of 30.4-nm flux have been made by Paresce et al. (refs. 5-17 and 5-18), Ogawa and Tohmatsu (ref. 5-19), and Young et al. (ref. 5-20). Although the distribution of the observed flux agrees broadly with the distribution that would be observed if the flux were due to scattering of solar 30.4-nm radiation off He II (singly ionized) trapped in the Earth's magnetosphere (Paresce et al., ref. 5-18), additional observations will refine knowledge of magnetospheric structure. Furthermore, a component of this flux scattered from the local ISM might exist. An observer within the Earth's lower magnetosphere could best detect such a component by observing from within the Earth's shadow, looking up the axis of the shadow. Positive identification of a local ISM component of 30.4-nm flux by this means would depend on detailed comparison of observations with models of the He II in the magnetosphere. Information about such a component would further clarify the interaction of the local ISM with the Sun's gravity and radiation and would facilitate correct inferences about distant ISM properties from local ISM observations. For this reason, the photometer was designed to observe local helium at both 58.4- and 30.4-nm wavelengths.

MISSION ENVIRONMENT

The Apollo-Soyuz Test Project (ASTP) helium glow detector (HGD) was mounted to a shelf inside one bay of the Apollo service module, approximately 1 m from the spacecraft main engine. The HGD observed through a remotely operated door that was closed for launch and opened in orbit during data takes. Previous Apollo flights and engineering studies had defined the environmental stresses to which the HGD would be subjected.

Although orbital flight imposed no mechanical loads on the HGD, it did contribute to several other environmental problems. Temperatures at the instrument attachment point were predicted to vary between 273 and 328 K (0° and 55° C). The HGD was required to operate successfully at temperatures set by these limits and by the varying radiant flux reaching the instrument through its

door. There was a possibility that gas leaks from another scientific instrument in the same bay might cause the local ambient pressure to rise from 0.1 to 1.0 N/m^2, which might have induced corona discharge from high-voltage elements of the HGD, resulting in possible damage to the instrument.

Degradation of the HGD optics would have occurred if they had become coated with contaminants that were purged or outgassed from Apollo systems. Transmission of extreme-ultraviolet (EUV) light at the wavelengths studied by the HGD is blocked almost completely by only 10 to 100 nm of most materials; and, in normal operation, the Apollo spacecraft exudes a diverse variety of contaminants.

The nominal 250-km altitude of the mission orbit placed the spacecraft well within the ionosphere and subjected the HGD to large fluxes of ions and electrons. The photon detectors used by the instrument respond to ions and electrons; therefore, the ionosphere fluxes posed a potential problem of severe data degradation.

DESIGN OF INSTRUMENT

The major systems of the HGD were photon detectors, broadband spectral filters, helium gas absorption cells and associated gas supply system, and electronic components.

Photon Detectors

The HGD included four photometers, each using a channel electron multiplier (CEM) as a photon detector. The photometers were generally similar in construction, operation, and performance to those discussed by Bowyer et al. (ref. 5-21). They featured a conical photocathode with an active diameter of 15 mm and an included angle of 22°, and a helical electron multiplier formed from capillary tubing. The fragile nature of these devices necessitated the development of a special mounting (Hoshiko, ref. 5-22).

Two identical channels were used to observe 58.4-nm radiation, and two more were primarily sensitive to 30.4-nm radiation. The band passes within which the photometers observed were defined by the EUV transmission of 80- to 160-nm-thick metal filters (Bowyer et al., ref. 5-21; and Steele, ref. 5-23). The 58.4-nm channels were used to view the sky through gas absorption cells, each of which was capped with one tin and one aluminum filter. Together, these filters provided a band pass approximately 10 nm wide, containing the 58.4-nm line. Each collimator for the 30.4-nm channels contained a single filter, composed of a layer of aluminum and a layer of carbon, which defined a similar band pass for this wavelength.

To prevent the CEM's from detecting charged ionospheric particles, the HGD used magnetic brooms to prevent ionospheric ions and electrons from entering photometer viewports and instrument-housing vents. Each broom was an annular array of magnets that produced a transverse magnetic field of approximately 15 mT (150 G), several centimeters in depth. Other possible locations for charged-particle leaks, such as joints and clearances around screws, were carefully sealed. A positive potential of 35 V was applied to the outer extremity of each CEM in normal operation, providing additional shielding against stray thermal positive ions.

Gas Absorption Cells

The dimensions of the helium gas absorption cells were selected so that each cell would contain an appropriate amount of gas; the thermal-Doppler-broadened helium scattering cross section near 58.4 nm was evaluated using an oscillator strength (Allen, ref. 5-24) of 0.276. Collisional broadening was not significant in the range of helium pressures and temperatures considered. Calculations indicated that a 0.1-m-long column of helium at a temperature of 300 K and a pressure of 130 N/m^2 absorbs more than 99 percent over a band approximately 3.5 pm full width, as shown in figure 5-1. Such a width is sufficient to absorb the geocoronal 58.4-nm line even when it is Doppler shifted by the 8-km/sec speed of an orbiting spacecraft.

Various mechanisms were considered that could reliably and repeatedly establish the design

pressure in the gas absorption cell in a flight instrument. Commercial regulators capable of delivering pressures of 100 to 200 N/m^2 reliably during a spacecraft mission were not available, nor were sensors for such pressures with sufficiently fast response to control a gas system by feedback.

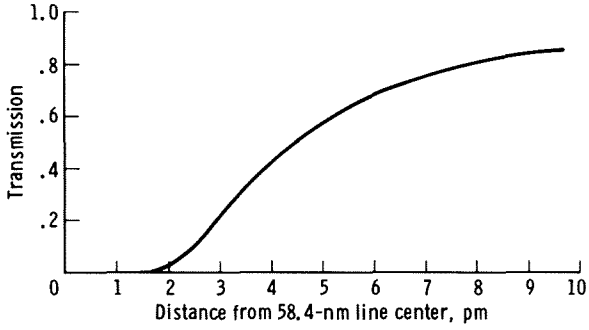

FIGURE 5-1.—Theoretical transmission of the filled gas absorption cell as a function of wavelength.

The system finally chosen for ASTP is shown in figure 5-2. Helium was supplied to the gas cells from a tank at a pressure of approximately 6 MN/m^2. The gas flowed through a master solenoid valve to a regulator, where its pressure was reduced to approximately 100 kN/m^2. The gas then flowed through adjustable needle valves into small transfer manifolds. To pressurize a gas cell, the fill valve was opened for a "preset" short interval, releasing into the cell the gas in the transfer manifold plus a small additional amount that leaked through the needle valve. The transfer manifold volume was selected so that it alone contained not quite enough helium to fill a cell to design pressure; and, during testing, the needle valve was adjusted until the total amount of gas released produced the desired pressure of 130 N/m^2.

A thermocouple gage tube was connected to each cell for continuous in-flight monitoring of cell pressure. A thermistor was bonded to each cell to measure cell temperature. The cells also served as collimators restricting the field of view of the 58.4-nm photometer channels to 14° full width half maximum. The collimators for the 30.4-nm channels were similar in mechanical design to the gas absorption cells and provided the same field of view.

Absorption cells for the Lyman-α line of atomic hydrogen, which are conceptually similar to the one described here but technically quite different, have been successfully used by Morton and Purcell (ref. 5-25), Winter and Chubb (ref. 5-26), and Blamont and Madjar (ref. 5-27). Helium absorption cells have been successfully flown by Delaboudiniere and Carabetain (ref. 5-28) in observations of the Sun, and by Freeman et al. (ref. 5-13) in studies of the local ISM.

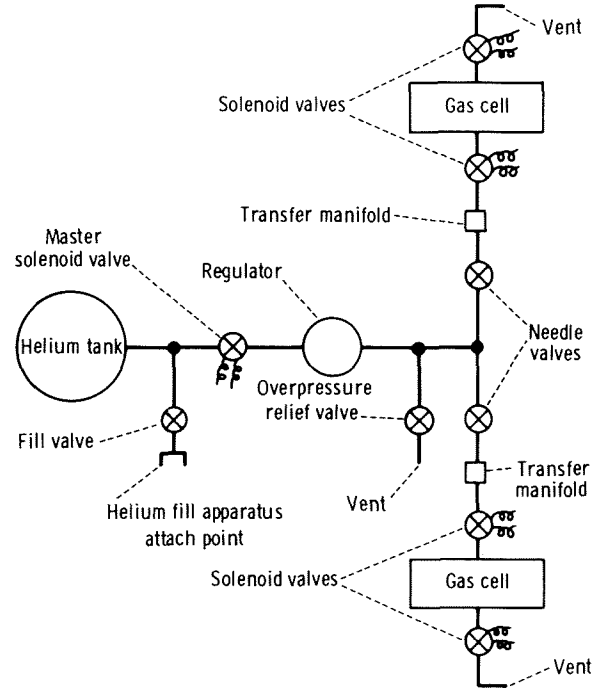

FIGURE 5-2.—Mechanical block diagram of HGD gas plumbing subsystem.

Thin Metal Filters

The mesh-supported thin metal filters used to restrict the photometer's broadband spectral response posed special design and development problems. Several filters were torn during initial vibration tests. The filter mounts were then

modified by providing an epoxy fillet between the filter surface and the interior of the mounting ring; the problem did not recur.

Thin metal filters mounted in flight configuration were tested to determine whether they could survive repeated application and removal of the 130-N/m^2 cell pressure. The test fixture used automatically controlled solenoid valves to apply and remove a preset, regulated differential pressure to a filter at a rate of approximately one complete cycle every 5 seconds. High-purity dry nitrogen gas was used to establish the pressure differential, and the tests were run at atmospheric pressure in a closed chamber that was continuously purged with high-purity dry nitrogen. The filters were visually inspected for pinholes before and after the test using backlighting under 10× magnification. Filter leak rates were measured with the test fixture before, during, and after the pressure cycling.

The number of gas absorption cell pressure cycles that each filter would undergo during calibration and flight was expected to be approximately 2.5×10^4. An aluminum-silicon filter was cycled 6.9×10^4 times. It showed no pinholes before or after testing. An upper bound for its leak rate at the conclusion of the test was 2×10^{-8} m^3/sec. If this leak rate were caused by a single round hole having a diameter greater than its length, the hole diameter would have been 2 μm. The leak rate corresponds to a pressure decay time constant (10^5 seconds) for helium leaking into a vacuum.

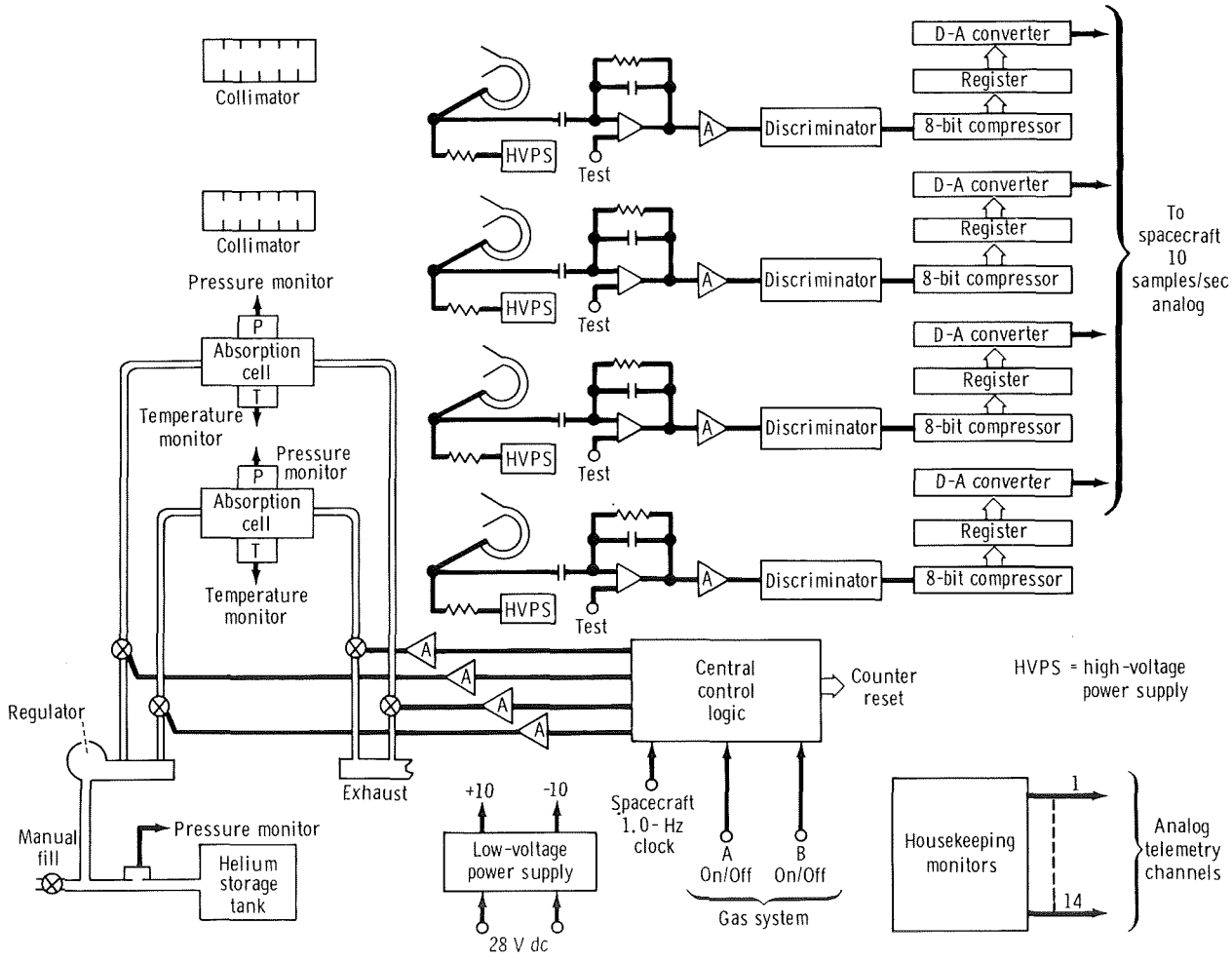

FIGURE 5-3.—Helium glow detector electronics subsystem block diagram.

A tin-germanium filter was cycled 9.0×10^4 times. It showed no pinholes before the test and five pinholes after test. The leak rate after testing was 2×10^{-7} m^3/sec, which corresponds to a single 6-μm-diameter hole and to a pressure decay time constant for helium leaking into vacuum of 10^4 seconds, which is still far longer than the 2.5-second interval during which the absorption cell was intended to hold pressure. Pinholes of these sizes could have caused only a negligible increase in background count rate, even when the instrument viewed the 2×10^{14} sec^{-1} m^{-2} (2×10^4 rayleighs) of Lyman-α flux from the daytime sky.

Electronics Subsystem

The HGD electronics subsystem is shown in block diagram form in figure 5-3. The amplifier system for each detector channel accepted signals as small as 10^{-14} C at a maximum random rate of 10^5/sec. A pulse-pair resolution of 1.0 microsecond ensured that statistical counting losses remained below 10 percent, even at maximum count rate.

The compressor and register for each channel accepted serial event pulses from the discriminator and produced an 8-bit output word representative of the number of events detected in each 0.1-second accumulation interval. The binary word was then converted by the digital-to-analog converter to an analog voltage compatible with the Apollo telemetry system. The output voltage was updated every 0.1 second in synchronization with the sampling of that voltage by the telemetry system.

Data compression was necessary because the 8-bit word used by the telemetry system allowed only 256 distinct output signals, whereas the event rates from the detector ranged up to 10^4 per sampling interval. An adaptive prescaler compression algorithm was selected that produced an output word the numerical value of which varied in a manner similar to the logarithm of the number of counts detected in the sampling interval.

The housekeeping parameters (gas absorption cell pressures, average absorption cell temperature, storage-tank gas pressure, and a current monitor for the high-voltage power supplies) were sampled and telemetered for real-time monitoring at Mission Control Center.

Timing and synchronization were controlled by the central control logic subsystem, which was synchronized to the spacecraft 1.0-Hz clock. The power system converted spacecraft 28 V dc power into various regulated low voltages for electronics subsystems and into regulated high voltages for the channel electron multipliers. To minimize single-point failures, each detector had an independent high-voltage supply.

Mechanical Features

The HGD was approximately a cube 0.35 m on each side with a mass of 21 kg. A general view of the instrument with the cover removed is shown in figure 5-4. The HGD was bolted into the Apollo spacecraft with thermally insulating mounts. The front face was coated with highly reflecting metallic tape to restrict radiative heating and cooling of the instrument. A black-coated shroud sealed the HGD to the inside of the spacecraft skin. The shroud restricted the flow of gases from the interior of the spacecraft service module into the HGD so that, when the instrument door was

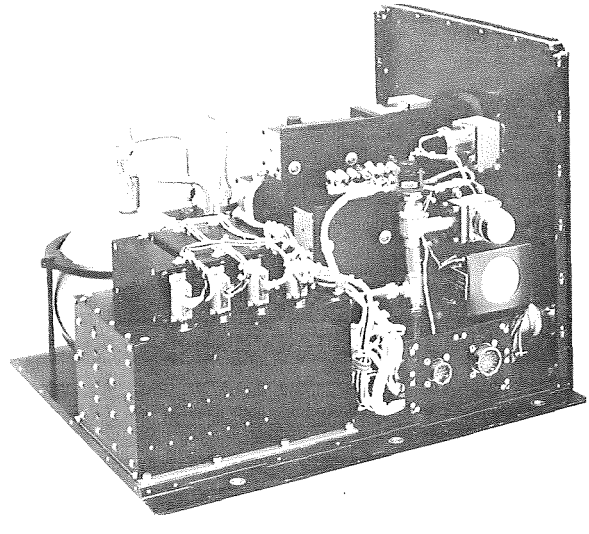

FIGURE 5-4.—Oblique view of HGD with cover removed. The optical axis points to the right.

opened, the instrument internal pressure fell to a value sufficiently low to prevent high-voltage corona discharge. The major characteristics of the HGD are summarized in tables 5-I and 5-II.

TABLE 5-I.—Helium Glow Detector Characteristics

Dimensions, m	0.33 by 0.33 by 0.43
Mass, kg	21
Average power, W	20
Gas cell pressure, N/m^2	130

TABLE 5-II.—Helium Glow Detector Channel Characteristics

Channel	*Design wavelength, nm*	*Nominal band pass, nm*	*Sensitivity at design wavelength, counts m^2 /photon*
1	58.4	50 to 70	15
2	30.4	20 to 50	140
3	58.4	50 to 70	18
4	30.4	20 to 50	140

INSTRUMENT CALIBRATION

The HGD was calibrated in the EUV calibration facility at the Space Sciences Laboratory of the University of California at Berkeley. This facility included a vacuum chamber, a grazing-incidence monochromator, several sources of EUV radiation, reference diodes for measuring ultraviolet and EUV fluxes, ion and electron guns, and such supporting equipment as pumps, manipulators, collimators, laminar-flow benches, and dehumidifiers.

The vacuum chamber had an inner diameter of 1.2 m and was 1.5 m long. An oil-diffusion pump with a liquid nitrogen cold trap provided sufficient pumping capacity to obtain a pressure of 1 to 0.1 mN/m^2, even when the HGD gas absorption cells were cycling. The chamber contained a remotely controlled manipulator that could translate the HGD in any direction perpendicular to its optical axis and simultaneously pitch and yaw it. The manipulator position was displayed on calibrated remote readouts.

A gas discharge lamp (Paresce et al., ref. 5-11), operated with various gases, provided a source of EUV light. The radiation passed through a 2.2-m McPherson grazing-incidence monochromator, a grazing-incidence paraboloidal collimator, and an adjustable stop, and then into the calibration tank. The monochromator was provided with its own diffusion pump and cold trap.

End-to-end photometric calibration of each detector channel was performed with emission lines of hydrogen, helium, neon, and argon (using a narrow, collimated monochromator output beam and a National Bureau of Standards calibrated vacuum photodiode as a reference standard). The beam intensities were adjusted to a sufficiently low level that statistical counting losses due to the 1-microsecond dead time of the CEM and electronics were insignificant. The resulting calibration curves are shown in figure 5-5.

The spatial shape of the photosensitive area of each channel was mapped at several wavelengths using a 1-mm-diameter collimated monochromator beam. The shape of each sensitive area agreed within the measurement error with the 13-mm-diameter clear aperture of each CEM. The response was constant across the region except for a small insensitive patch at the center of the CEM, where the electron-multiplier section of the device joins the photoemissive surface. This insensitive patch accounted for only a few percent of the total CEM area.

The shape of the solid angle viewed by each channel was studied by varying both the angle that the incident photon beam made with the detector optical axis and the position of the beam in the channel entrance pupil. The response remained constant as long as the beam directly illuminated the CEM. When the beam did not directly illuminate the CEM but instead reached it after one or more reflections off the interior of the gas absorption cell or collimator, the response never exceeded 5×10^{-3} of the direct response. Calculations indicated that, if each channel viewed an isotropic source of radiation to which it was sensitive, no more than 3 percent of the photons detected would have reached the detector by such reflections.

The photometric linearity of each channel was examined and was found to be consistent with that calculated from the Poisson statistics of photon arrival together with the known 1-microsecond dead time of the detector electronics following each event. In the laboratory, the dark rate of each channel was found to be less than 0.1 count/sec. This rate is consistent with that expected from false counting due to cosmic radiation.

The gas absorption cells were operated to verify that their pressure cycling had the correct amplitude, frequency, and phase. The pressure sensors for these measurements were those contained in the HGD, which had been separately calibrated in helium before assembly.

A source of ions and electrons could be mounted in the calibration tank to determine whether the HGD would respond when exposed to ionospheric charged particle fluxes. The source was a high-perveance vacuum diode composed of a resistance-heated nichrome/barium oxide filament, a cylindrical mesh anode, and a surrounding electrostatic focus cup at anode potential. The diode was capable of producing up to 2×10^{10} positive ions/sr • sec, or up to 2×10^{14} electrons/sr • sec at energies up to approximately 400 eV. The source geometry was approximately that of a point source radiating into 1 sr of solid angle. The source was mounted approximately 0.1 m from the instrument and the HGD was then translated vertically and laterally to present its entire front face to the flux of particles.

The maximum flux of positive ions produced by the source (2×10^{10} ions/sr • sec) did not raise any HGD count rate above background. On this basis, an upper limit to the integral of effective area over solid angle for 200-eV ion sen-

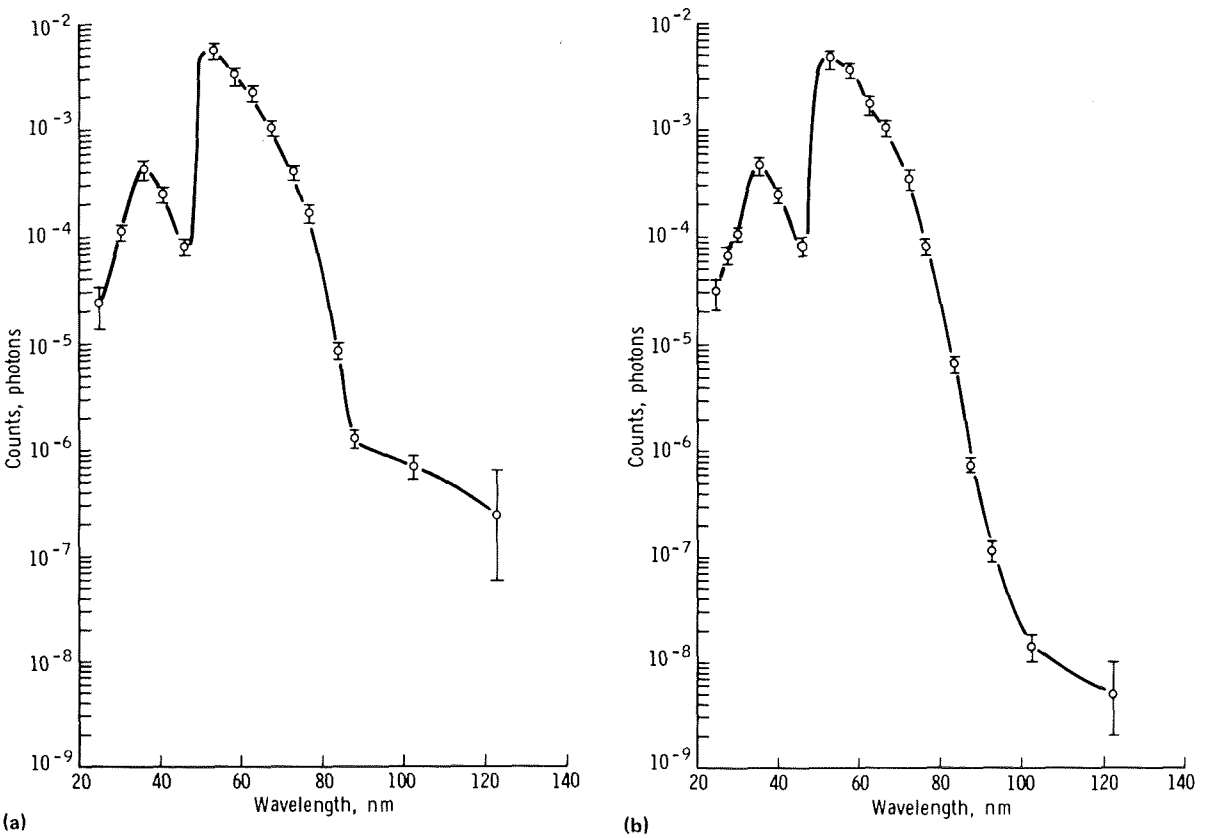

FIGURE 5-5.—Absolute end-to-end sensitivity of HGD channels as a function of wavelength. (a) 58.4-nm channel no. 1. (b) 58.4-nm channel no. 3. (c) 30.4-nm channel no. 2. (d) 30.4-nm channel no. 4.

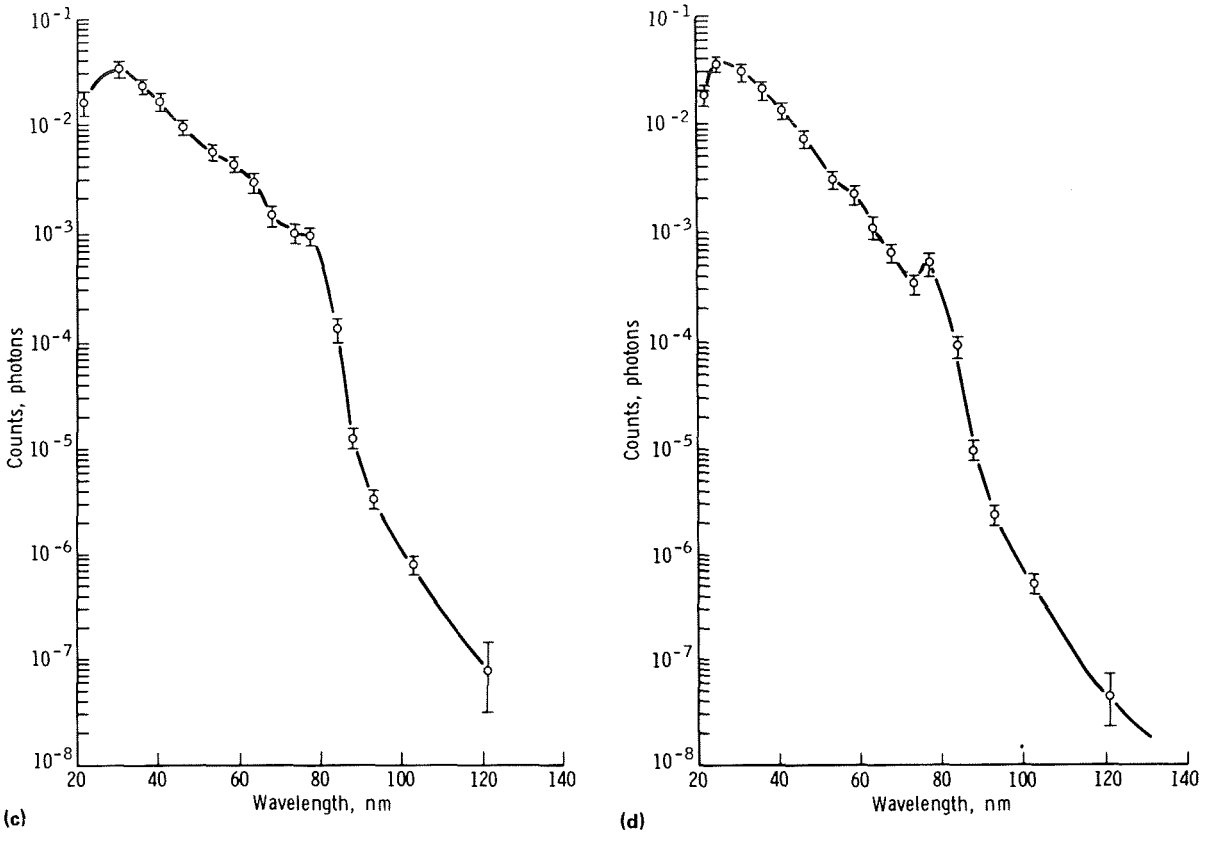

FIGURE 5-5.—Concluded.

sitivity of each HGD channel was calculated to be 10^{-12} m^2 • sr. A much larger electron flux of 2×10^{14} sr^{-1} sec^{-1} was generated by the source. This flux was detectable and gave integrals of effective area over solid angle for 10-eV electrons for the various channels of 10^{-17} to 10^{-16} m^2 • sr.

One vent port in the front face of the HGD allowed the internal volume of the instrument to outgas to space. This port was baffled internally. An intense beam of 58.4-nm photons was directed into the port and all count rates were monitored to investigate the possibility that a combination of internal reflections and photoemission inside the instrument might cause false counts. The sensitivities detected by this method ranged from 2.7×10^{-9} to 1.6×10^{-8} counts detected per photon passing into the vent port. A similar test using a source that approximated the luminous flux of the Sun, but at a lower black-body temperature of approximately 3000 K, yielded no count rate significantly above background.

An intense 58.4-nm beam was used to illuminate each of the four detectors serially, and the count rates of all four channels were simultaneously monitored. The amounts of crosstalk observed ranged from 1.1×10^{-9} to 6.0×10^{-9} counts in an unilluminated channel (per photon entering the entrance pupil of a different channel).

FLIGHT OPERATIONS

The HGD and its protective door were controlled by switches and circuit breakers in the Apollo command module. The crewmembers also controlled a switch that could interrupt the flow of

helium to either gas absorption cell. This switch could have been used if declining tank pressure or corona discharge had indicated a leak in either gas cell. When observations were to be made, the crewmembers opened the door, waited a few moments to allow the pressure in the instrument area to drop from 0.1 to 1.0 N/m^2 (door closed) to 1 mN/m^2 or less (door open), and turned on the power. The short wait before turn-on was necessary to avoid possible corona discharge from the high-voltage electronics at pressure above 0.1 N/m^2.

The door was never opened within 15 minutes after the completion of any discrete purge or vent of contaminants from the spacecraft. Dynamical calculations based on residual atmospheric drag at an altitude of 250 km indicated that a 15-minute delay was adequate to allow even contaminant particles as large as 0.01 m in diameter to drift clear of the spacecraft. Furthermore, crewmembers engaged in extravehicular activity on previous Apollo missions have not observed ice crystals or other contaminants clinging to the spacecraft near the location of the HGD.[1]

Four Apollo reaction-control thrusters located close to the HGD were inhibited from firing during HGD observations. The high level or redundancy of the Apollo attitude control system allowed the spacecraft to maneuver properly with the 12 remaining thrusters.

The HGD was pointed at various areas of the sky by maneuvering the spacecraft. These maneuvers were carefully planned before the flight and consisted, for the most part, of slow rolls about the spacecraft long axis, with that axis pointing in a specified fixed direction. For each axis orientation chosen, the spacecraft was rolled through several short arcs that together spanned the complete great circle normal to the axis. The times at which the various rolls were made were selected so as to minimize the zenith angles of the observations and to maximize the portion of the data taken with the spacecraft in darkness.

The observations maneuvers selected allowed the instrument to survey over three-quarters of the celestial sphere. Furthermore, the maneuvers were chosen to permit especially detailed and repeated study of the region where the pronounced helium-density variations mentioned previously occur, and of the portion of sky that can be viewed while looking down the shadow cast by the Earth in the geocorona.

Data useful for in-flight checks of instrument calibration and sensitivity to unwanted wavelengths of light were taken while the instrument viewed the Earth and the horizon. At the last turn-off of the HGD, the instrument was intentionally operated with the door closed to check the background count rate with no light reaching the detectors.

RESULTS

The HGD returned approximately 10 hours of data, including approximately 2 hours devoted to a systematic survey of half the celestial sphere. Previously developed software was used for reduction and rough analysis of the data. The immediate conclusions were as follows.

1. One 30.4-nm detector failed part way into the mission.
2. All functioning detectors exhibited unexpectedly high count rates when the Sun was above the horizon.
3. All functioning detectors yielded nighttime count rates that were generally comparable to previous measurements of 58.4- and 30.4-nm nighttime flux.
4. One 58.4-nm detector occasionally gave a count rate substantially higher than the other 58.4-nm detector. The variation of this count rate with spacecraft position and line-of-sight orientation suggested that detector number 1 had acquired an unwanted sensitivity to Lyman-α radiation at 121.6 nm.
5. Door-closed dark counting rates did not exceed 0.1 count/sec.

The objective of further reduction of 58.4-nm data has been to determine parameters of the local ISM by evaluating the chi-squared polynomial, comparing the observations with predictions made using present ISM models. The subset of cell-empty data (taken when the Sun was more than 30° below the horizon, when the line-of-sight

[1]Personal communications, R. Evans, 1974.

was within 60° of the zenith, and when the spacecraft was well clear of the highly charged particle fluxes in the South Atlantic Anomaly) was selected for more complete analysis.

The 53 minutes of these data were binned in 30-second intervals, using a filtering process that rejected individual data samples that were more than 3 standard deviations above or below the average sample size for the bin. The purpose of this filtering process was to ensure that the reduced data were free of spurious signals, such as might be caused by electronic noise in the telemetry system. The preliminary reduction was performed without taking into account any corrections due to absorption of 58.4-nm flux by the Earth's atmosphere above the spacecraft.

Existing ISM models were then used to calculate predicted flux levels for these observations, as a function of ISM model parameters. The chi-squared polynomial comparing prediction to observation was evaluated for each set of parameters considered. No satisfactory fit was obtained, indicating that the existing models, without correction for atmospheric absorption, did not adequately explain the observations.

The chi-squared polynomial was then reevaluated for the 17.5-minute subset of the previous data set for which the line-of-sight lay within 30° of the zenith. The best fit obtained was much better, though still not adequate to explain the observations. The chi-square fits obtained are summarized in table 5-III. The observed isophotes for the 17.5-minute data set together with the corresponding predicted isophotes for the best fit to these data are displayed in figure 5-6.

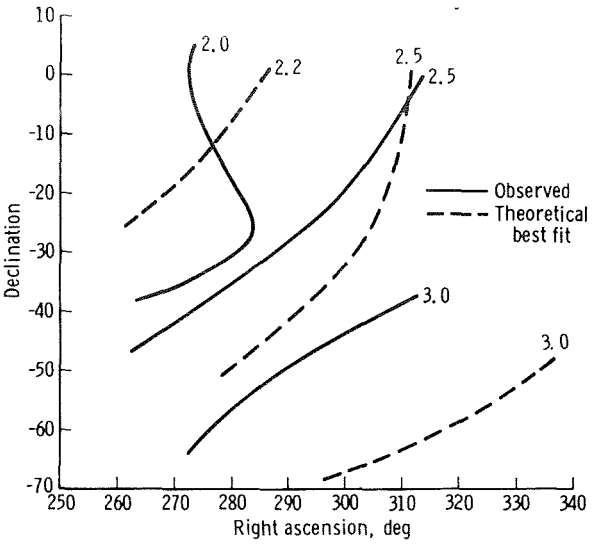

FIGURE 5-6.—Preliminary observed isophotes and best-fit theoretical isophotes for the 17.5-minute data set. (Isophotes parameterized by rayleighs.)

ACKNOWLEDGMENTS

Robert Stern, Stanford University, assisted with calibration and integration. The instrument and its ground support equipment were fabricated by Ball Brothers Research Corporation.

TABLE 5-III.—Preliminary Fits of Cold ISM Models to Subsets of Experiment Data

Zenith angles at which data were taken, deg	*Data points, no.*	*Degrees of freedom, no.*	*Chi square per degree of freedom*
0 to 60	106	102	28.8
0 to 30	35	31	11.5

REFERENCES

5-1. Danby, J. M. A.; and Camm, G. L.: Statistical Dynamics and Accretion. Monthly Notices Roy. Astron. Soc., vol. 117, 1957, pp. 50-71.

5-2. Blum, P. W.; and Fahr, H. J.: Interaction Between Interstellar Hydrogen and the Solar Wind. Astron. & Astrophys., vol. 4, 1970, pp. 280-290.

5-3. Holzer, T. E.; and Axford, W. I.: Interaction Between Interstellar Helium and the Solar Wind. J. Geophys. Res., vol. 76, Oct. 1971, pp. 6965-6970.

5-4. Axford, W. I.: The Interaction of the Solar Wind With the Interstellar Medium. Solar Wind. NASA SP-308, 1972, pp. 609-660.

5-5. Johnson, H. E.: Backscatter of Solar Resonance Radiation - I. Planet. & Space Sci., vol. 20, June 1972, pp. 829-840.

5-6. Wallis, Max K.: Local Hydrogen Gas and the Background Lyman-Alpha Pattern. Monthly Notices Roy. Astron. Soc., vol. 167, 1974, pp. 103-119.

5-7. Thomas, G. E.; and Krassa, R. F.: OGO 5 Measurements of the Lyman Alpha Sky Background. Astron. & Astrophys., vol. 11, 1971, pp. 218-233.

5-8. Bertaux, J. L.; and Blamont, J. E.: Evidence for a Source of Extraterrestrial Hydrogen Lyman-Alpha Emission: The Interstellar Wind. Astron. & Astrophys., vol. 11, 1971, pp. 200-217.

5-9. Thomas G. E.: Properties of Nearby Interstellar Hydrogen Deduced From Lyman-α Sky Background Measurements. Solar Wind. NASA SP-308, 1972, pp. 668-683.

5-10. Paresce, Francesco; Bowyer, Stuart; and Kumar, Shailendra: Evidence for an Interstellar or Interplanetary Source of Diffuse He I 584 Å Radiation. Astrophys. J., vol. 183, July 1973, pp. L87-L90.

5-11. Paresce, F.; Kumar, S.; and Bowyer, C. S.: Continuous Discharge Line Source for the Extreme Ultraviolet. Appl. Opt., vol. 10, no. 8, 1971, pp. 1904-1908.

5-12. Weller, C. S.; and Meier, R. R.: Observations of Helium in the Interplanetary/Interstellar Wind: The Solar-Wake Effect. Astrophys. J., vol. 193, Oct. 1974, pp. 471-476.

5-13. Freeman, J.; Bowyer, S.; Paresce, F.; and Lampton, M.: Gas Absorption Cell Photometer for Rocket Observations of Local Interstellar Helium. Rev. Sci. Instrumen., vol. 47, Mar. 1976, pp. 227-281.

5-14. Fahr, H. J.: The Extraterrestrial UV-Background and the Nearby Interstellar Medium. Space Sci. Rev., vol. 15, Feb. 1974, pp. 483-540.

5-15. Jacchia, L. G.: Revised Static Models of the Thermosphere and Exosphere With Empirical Temperature Profiles. SAO-SR-332, Smithsonian Institution Astrophysical Observatory, Cambridge, Mass., 1971.

5-16. Thomas, G. E.: Interplanetary Gas of Nonsolar Origin. Rev. Geophys. Space Phys., vol. 13, July 1975, pp. 1063-1065.

5-17. Paresce, Francesco; Bowyer, C. Stuart; Kumar, Shailendra; and Lampton, Michael: Rocket Observations of Extreme Ultraviolet Radiation in the Night Airglow. EOS, Trans. A.G.U., vol. 51, 1970, p. 795.

5-18. Paresce, F.; Bowyer, S.; and Kumar, S.: Observations of the He II 304-A Radiation in the Night Air. J. Geophys. Res., vol. 78, Jan. 1973, pp. 71-79.

5-19. Ogawa, Toshihiro; and Tohmatsu, Takao: Sounding Rocket Observation of Helium 304- and 584-Å Glow. J. Geophys. Res., vol. 76, Sept. 1971, pp. 6136-6145.

5-20. Young, James M; Weller, Charles S.; Johnson, Charles Y.; and Holmes, Julian C.: Rocket Observations of the Far UV Nightglow at Lyman α and Shorter Wavelengths. J. Geophys. Res., vol. 76, June 1971, pp. 3710-3722.

5-21. Bowyer, C. S.; Lampton, M.; Mack, J.; and Paresce, F.: A Far Ultraviolet Photometer for Space Research. Planet. & Space Sci., vol. 18, June 1970, pp. 835-845.

5-22. Hoshiko, H. H.: Helical Channel Multiplier Package Design for Space Instrumentation. Rev. Sci. Instrumen., vol. 46, Mar. 1975, pp. 331-332.

5-23. Steele, Gordon N.: Development and Fabrication of Large-Area Extreme-Ultraviolet Filters for the Apollo Telescope Mount. Space Optics. B. J. Thompson and R. R. Shannon, eds., National Academy of Sciences (Washington, D.C.), 1974, pp. 367-389.

5-24. Allen, C. W.: Astrophysical Quantities. Third ed. University of London, 1973, p. 72.

5-25. Morton, Donald C.; and Purcell, J. Dewitt: Observations of the Extreme Ultraviolet Radiation in the Night Sky Using an Atomic Hydrogen Filter. Planet. & Space Sci., vol. 9, Aug. 1962, pp. 455-458.

5-26. Winter, Thomas C. Jr.; and Chubb, Talbot A.: The Determination of the Profile of the Night Sky Hydrogen Lyman Alpha Emission Line. J. Geophys. Res., vol. 72, Sept., 1967, pp. 4405-4414.

5-27. Blamont, J. E.; and Madjar, A. Vidal: Monitoring of the Lyman Alpha Emission Line of the Sun During the Year 1969. J. Geophys. Res., vol. 76, July 1971, pp. 4311-4324.

5-28. Delaboudiniere, J. P.; and Carabetian, C.: A Rocket Borne Absorption Cell for High Resolution Spectroscopy of the He I Line at 584 Å for Solar Observations. Space Sci. Instrumen., vol. 1, Feb. 1975, pp. 91-110.

BIBLIOGRAPHY

Canfield, L. R.; Johnston, R. G.; and Madden, R. P.: NBS Detector Standards for the Far Ultraviolet. Appl. Opt., vol. 12, no. 7, 1973, pp. 1611-1617.

Wallis, M. K: Interaction Between the Interstellar Medium and Solar Wind Plasma. Astrophys. and Space Sci., vol. 20, Jan. 1973, pp. 3-18.

Wallis, Max K.: Collisional Heating of Interplanetary Gas: Fokker-Planck Treatment. Planet. & Space Sci., vol. 23, Mar. 1975, pp. 419-430.